# ANALYSIS OF THE ST-T COMPLEX OF THE ELECTROCARDIOGRAM USING THE KARHUNEN-LOEVE TRANSFORM: ADAPTIVE MONITORING AND ALTERNANS DETECTION

February 4, 1999

by


Pablo Laguna, Ph.D., Member IEEE (*)
George B. Moody, Member IEEE (&)
José García (*)
Ary L. Goldberger, MD (#)
Roger G. Mark, Ph.D., MD., Senior Member IEEE (&)

(*) Grupo de Tecnologías de las Comunicaciones
Departamento de Ingeniería Electrónica y Comunicaciones
Centro Politécnico Superior
Universidad de Zaragoza.
Zaragoza, SPAIN.

(&) Division of Health Sciences and Technology
Harvard - Massachusetts Institute of Technology
Cambridge, MA. U.S.A.

(#) Cardiovascular Division
Beth Israel Hospital - Harvard Medical School
Boston, MA. U.S.A.

*Address for correspondence:*

(*) Departamento de Ingeniería Electrónica y Comunicaciones
Centro Politécnico Superior. Universidad de Zaragoza
C/ Maria de Luna 3,
50015 Zaragoza
SPAIN.

Telephone: 34-976-761931
FAX: 34-976-762111
e-mail: laguna@posta.unizar.es


## ACKNOWLEDGEMENTS


This work was supported in part by project TIC97-0945-C02-02 from CICYT, a personal grant to P.L. from the "Instituto Aragones de Fomento (IAF)" (Spain) and by grants from the G. Harold and Leila Y. Mathers Charitable Foundation and the National Aeronautics and Space Administration (USA).

**Abstract**

The Karhunen-Loève transform (KLT) has been applied to study the ventricular repolarization period as reflected in the ST-T complex of the surface ECG. Characterisation of the repolarization period (which may contain subtle evidence of cardiac electrical instability) must take account of the entire ST-T period. We have used the KLT as a sensitive means of quantizing ST-T shape with an overall index, the *kl* coefficients. Since the KLT is signal dependent, we assembled a diverse set of roughly 100,000 ST-T complexes from 105 fifteen-minute excerpts of digitized two-channel ambulatory ECG recordings. First, using uniformly sampled ST-T complexes, we derived a set of KLT basis vectors that permit representation of 90% of the signal energy using 4 KLT coefficients for each ST-T complex. In a second experiment, Bazett's correction was used to normalize the ST-T duration, after which a second set of KLT basis vectors was derived which was more efficient in signal representation. Since a truncated KLT expansion tends to favour representation of the signal over any additive noise, a time series of KLT coefficients, obtained from successive ST-T complexes, is better-suited for representation of both medium-term variations in ST-T morphology (such as ischemic changes) and short-term variations (such as ST-T alternans) than discrete parameters such as ST level or other local indexes. For analysis of ischemic changes, we describe an adaptive filter that may be used to estimate the KLT coefficients, yielding an increase in signal-to-noise ratio of 10 dB ($\mu = 0.1$), with a convergence time of about 3 beats. We use a beat spectrum of the UN-filtered KLT coefficient series for detection of ST-T alternans. Finally, we illustrate these methods with examples from the European ST-T Database obtaining that about 20% of records at the database reveal a quasi-periodic salvos pattern of ischemic (or ST-T changes) episodes and other 20% exhibit repetitive but not clearly periodic patterns of ST-T change episodes. It has been obtained that about 5% of ischemic episodes present alternans associated with them.

**Keywords**: ST level, ST-T complex, Ischemia, KL Transform, Alternans, Monitoring.

# 1 Introduction

Electrocardiographic (ECG) information is derived from analysis of both the depolarization (QRS complex) and repolarization (ST-T waveform) phase of the cardiac electrical cycle. Considerable interest has been directed at ventricular repolarization (VR) in recent years because subtle ST-T changes may be a marker of electrical instability that might result in increased susceptibility to ventricular fibrillation (VF), and sudden cardiac death (SCD) (Rosenbaum et al., 1994). Repolarization may be perturbed by multiple factors including ischemia, structural heart disease, metabolic factors (e.g. electrolyte abnormalities, drugs) and neurohumoral factors.

At present, there are no generally accepted non-invasive indices of the risk of SCD, although such indices would have very substantial implications for both public health policy and medical practice, and many

studies have sought to develop such indices. Among the most promising candidates are measurements of heart rate variability (HRV) (Klieger et al., 1984; Myers et al., 1986), ventricular late potentials (Berbari and Lazzara, 1988; Breithardt et al., 1991), repolarization duration (QT) interval (Puddu and Bourassa, 1986), QT variability (Merri et al., 1993; Speranza et al., 1993), assessment of heterogeneity of repolarization (Q-T interval) in different leads, and repolarization alternans (Clancy et al., 1991; Rosenbaum et al., 1994) (a possible precursor of ventricular fibrillation). Except for the first two, all of these indices are derived from the ST-T complex of the ECG, which has long been known as a highly sensitive (though arguably less predictive) marker of myocardial ischemia (Gallino et al., 1984; Akselrod et al., 1987).

Most of these indices to describe VR are derived from discrete features of the ST-T complex, a practice that reflects the difficulty of deriving integrated measurements using visual analysis. However the ST-T waveform represents a complex spatial and temporal summation of electrical potentials from innumerable ventricular cells. Therefore, if physiologically and clinically relevant information is contained within the ST-T complex, this information may not necessarily be concentrated within any individual differential feature or subinterval such as ST levels and QT intervals, but may be represented by the entire ST-T waveform. The proliferation of additional "heuristic" measurements that describe the ST-T complex shape clearly demonstrates the need to consider more than the traditional measurements in order to characterize subtle changes in VR. Furthermore, noise and other sources of measurement error (such as errors in fiducial or baseline estimation) have far more deleterious effects on measurements of isolated features and simple differential measurements than on integrated measurements. These considerations, together with the increasing evidence for the importance of repolarization alterations as a marker of electrical instability and SCD, led us to consider the objective of developing an analytic technique based on the entire ST-T complex.

We chose to use the Karhunen-Loève transform (KLT) which has the power to characterize the shape of the entire ST-T complex, and which is minimally affected by noise. We propose that a feature set of KLT coefficients would provide a superior method for characterizing each beat, and that the KLT feature set would provide a much more sensitive and robust quantization of ST-T shape than the discrete measures commonly used in clinical practice, like ST or QT measures. In a previous study (Jager et al., 1992), the KLT was successfully applied to analyze the ST segment of the ECG, with the specific aim of obtaining noise-tolerant methods for ischemia detection. In this study, we have applied the KLT to the entire ST-T complex, in order to include as much information about VR as possible, with the broader aim of noise-tolerant characterization of both beat-to-beat and longer-term variations in VR.

In the following sections, we describe our technique for ST-T complex representation, including construction of KLT basis functions and derivation of $\mathrm{KL}_n$ coefficient time series, $kl_n(i)$. We also present an adaptive filter (Laguna et al., 1996a; Thakor et al., 1993), suitable for estimating the $kl_n(i)$

time series, that reduces the noise of the $kl_n(i)$ estimation while preserving the deterministic coefficient information. We apply these techniques to ECG records from the European ST-T Database, and we show how the first and second $kl_n(i)$ $(n = 1, 2)$ series may be used to monitor ST segment changes in these records. We illustrate this point with examples of periodic behaviour of the ischemic process within these records. We also analyze the power spectral density (PSD) of the $kl_n(i)$ series. This analysis is done using PSD estimation of the $kl_n(i)$ coefficients expressed with temporal reference the beat order (DeBoer et al., 1984) (as previously used for HRV analysis) rather than the beat occurrence time $t_i$. This analysis also points out the possibility of detecting ventricular alternans using the peaks of the spectrum at 0.5 $beat^{-1}$ "beatquency". We show examples (from the European ST-T Database) of the appearance of alternans in association with ischemic ST and T-wave changes, which were successfully detected by this method.

## 2 The Karhunen-Loève transform applied to the ST-T complex

The KLT (Haddad and Parsons, 1991) is a signal-dependent linear transform that is optimal in the following sense: for a given signal (an ST-T complex) lasting N samples and any given number of parameters $n \leq N$, if the signal is reconstructed from the first $n$ terms of the series expansion of a linear transformation, the lowest expected mean-squared error will be obtained if the transform is chosen to be the KLT. The KLT thus has two major advantages over other linear transforms: it concentrates the signal information in the minimum number of parameters, and it defines the domain where the signal and noise are most separated. These properties are obtained at the expense of generality, however: it is by estimation of the "most likely" variations in waveform shape that the KLT acquires its property of noise rejection. A KLT for a given type of signal must be derived from the statistics of examples of that signal; it is unlikely to be useful (with the same optimal properties) for analysis of other types of signals. Thus, a significant constrain of the KLT is that it is necessary to collect a representative "training" set of the signals to be analyzed, in order to derive the KLT basis functions (eigenfunctions). The performance of the KLT, in terms of capacity to concentrate information in a small coefficient set, depends on how well the training set has been constructed. Once each ST-T complex is characterized by $n$ $kl$ coefficients we construct $n$ $kl$ series $(kl_n(i))$ as the series formed by the $kl$ coefficients of the $ith$ beat.

In this section we describe our technique for analyzing the ST-T complex using the KLT. First we discuss the derivation of the training set, including the preprocessing performed on the ECG to attenuate noise and to exclude beats likely to be significantly corrupted by noise. We then present an adaptive filter for estimating the $kl_n(i)$ series of an ECG record.

In this work, we represent each ST-T complex first by a *pattern vector*, $\mathbf{x}$, whose components are the time-ordered samples of the ST-T complex (after baseline correction and normalization, described below). The KLT is a rotational transformation of a pattern vector into a *feature vector*, whose components are

the KLT coefficients. As shown below, the first few components of the feature vector represent almost all of the signal energy, and the remaining components need not even be computed.

The derivation of the KLT basis functions begins by estimating the covariance matrix $\mathbf{C}$ of the pattern vectors of the training set (Haddad and Parsons, 1991),

$$\mathbf{C} = E\{(\mathbf{x} - \mathbf{m})(\mathbf{x} - \mathbf{m})^T\} \tag{1}$$

where $\mathbf{m}$ is the mean pattern vector over the entire training set. The covariance matrix reflects the distribution of the pattern vectors in the pattern space. The orthogonal eigenvectors of $\mathbf{C}$ are the basis functions of the KLT, and the eigenvalues, $\lambda_k$, represent the average dispersion of the projection of a pattern vector onto the corresponding basis function. After sorting the eigenvectors in order by their respective eigenvalues, such that $\lambda_k \geq \lambda_{k+1}$, for $k = 0, 1, ...., N-1$, the corresponding basis functions are arranged in order of representational strength. The basis function corresponding to the largest eigenvalue is that function best able to represent an arbitrary pattern vector from the training set; the next function is the (orthogonal) function best able to represent the residual error obtained from fitting the first function, etc. The value of $N$ is equal to the number of components in the pattern vector, and depends on the length of the waveform and on the sampling frequency; in this case the length is 600 ms, and the sampling frequency is 250 Hz, so that $N = 150$.

In this study, the mean pattern vector $\mathbf{m}$ can be forced to be zero, if we assume that each ST-T complex in the training set can represent both itself and its inverted counterpart. This represents the possibility that any ST-T complex may appear inverted simply as an artifact of the choice of the lead polarity when recording the ECG. Thus, the covariance matrix may be expressed simply as

$$\mathbf{C} = E\{(\mathbf{x})(\mathbf{x})^T\} \tag{2}$$

and the eigenvalues, rather than representing the average dispersion of the ST-T projection onto the associated basis function, instead represent the average energy of this projection.

## 2.1 Derivation of the training set and the $KL_n$ basis functions

To obtain a representative training set of normal and abnormal ST-T waveforms we selected a wide variety of ECG records, 105 in all (Laguna et al., 1997) (15 from the MIT-BIH Arrhythmia Database (Moody and Mark, 1990a), 6 from the MIT-BIH ST Change Database, 13 from the MIT-BIH Supra-ventricular Arrhythmia Database, 10 recordings of healthy subjects from BIH, 33 from the European ST-T Database (Taddei et al., 1992), 4 from the MIT-BIH Long-Term Database and 24 from SCD recordings collected at BIH) which included a wide spectrum of T-wave shapes, ST elevation, ST depressions, etc. From each of these 105 recordings, a 15-minute excerpt was selected. Since the noise discrimination power of the KLT

depends on the distribution of the pattern vectors as reflected in the covariance matrix, we tried to avoid including segments that were obviously corrupted by baseline wander or other noise.

From these 105 fifteen-minute records, we selected the training set of ST-T complexes according to the following procedure. First, QRS complexes were detected and labeled using ARISTOTLE software (MOODY AND MARK, 1982). Each detected QRS complex was marked at a fiducial point corresponding to the centre of gravity of the significant peaks of the convolution of the QRS complex with the QRS detection function, a matched filter characterized by a W-shaped impulse response. This method of fiducial point placement was chosen for its stability with respect to minor morphology changes, as in respiration-related axis shift, as well as for its tolerance of impulse noise. The QRS fiducial points generally coincide with the R-wave peaks of monophasic QRS complexes, and lie between the major positive and negative deflections of biphasic QRS complexes. We defined the ST-T complex as the portion of the signal within a window beginning 85 ms following a QRS mark, $q_i$, and ending 240 ms prior to the next QRS mark, $q_{i+1}$. If the RR interval, $rr_i$ (defined as the interval between the QRS marks), is less than 720 ms, the end of the window is located at $q_i + \frac{2}{3}rr_i$ (i.e., 2/3 of the way from the initial QRS mark to the following one). This strategy permits inclusion of the whole ST-T complex, independently of the QT duration. (The ST-T window is restricted to 600 ms.) In those cases when T waves end later than 240 ms prior to the next QRS mark it is very likely that T waves are distorted by the next P wave. It is better to exclude those beats rather than have them corrupt the training set. These values have been selected according to the clinical values of intervals and from our experimental work when deriving the KLT of the ST-T complex. When we refer to ST-T as defined here we include the U wave, in the cases where it exists. This will be observed later when discussing Fig. 2 . *Fig.* 2

To avoid the effects of ectopic and other abnormal beats on the ST-T complex, we accepted only ST-T complexes associated with QRS complexes labelled as normal by ARISTOTLE (MOODY AND MARK, 1990B), and further required that both the previous and following QRS complexes also be labelled as normal. For each beat, we estimated the isoelectric level in the PR interval as the signal averaged during the 20 ms interval beginning 80 ms prior to the QRS mark. This isoelectric value, measured in the different beats, was used as input to the cubic splines interpolation of the ECG signal in the baseline cancellation (MEYER AND KEISER, 1977). Beats for which the estimated isoelectric level differed by more than 0.2 mV from that of the previous or following beat were excluded from the training set. The presence of delta waves associated with pre-excitation (Wolff-Parkinson-White syndrome) in four records required us to use intervals beginning 100 ms (records *sel50*, *sel308*, and *sel17152*) or 120 ms (record *sel230*) prior to the QRS mark for the isoelectric level estimation in these cases. We then manually rejected a small number of ST-T complexes we judged subjectively to be particularly noisy. The remaining 97,663 ST-T complexes formed the training set.

We generated the set of pattern vectors for the training set in six different ways, to test the effects of

ST-T dependence on heart rate (HR) and of noise on the KLT representation. We used both uniformly sampled ST-T complexes, and complexes corrected with Bazett's formula (Bazett, 1920) and resampled. We corrected for baseline variation using cubic splines and using a high-pass filter. (Since the KLT basis functions will be influenced by incorrectly determined isoelectric levels, we selected recordings with minimal baseline variation. Even in such recordings, however, it is still necessary to account for baseline variation caused by respiration.) Finally, given the low-frequency content of the ST-T complex (Thakor et al., 1984), we have also studied the effects of bandpass filtering the ECG signal as a means of improving the signal-to-noise ratio. These considerations led us to develop six sets of pattern vectors from the training set:

1 Using cubic splines for baseline removal (Meyer and Keiser, 1977). The knots were taken to be the centres of the isoelectric intervals, as defined above.

2 As in set 1, but correcting for the effects of heart rate on the ST-T complex using Bazett's formula. This is performed by re-sampling within the ST-T window at a sampling frequency equal to the original (250 Hz) divided by $\sqrt{rr_i}$, where $rr_i$ is the previous RR interval and is expressed in seconds. The result is a corrected ST-T complex, $STT_c(t') = STT(t/\sqrt{rr_i})$.

3 Using a second-order high-pass filter (Lynn, 1977) with a cut-off frequency of 1 Hz for baseline removal.

4 As in set 3, but with HR correction as in set 2.

5 Using bandpass filtering: a high-pass filter as in set 3, together with a second-order low-pass filter (-3 dB at 28 Hz) for attenuation of high-frequency noise.

6 As in set 5, but with HR correction as in set 2.

In each case, the pattern vectors were normalized by magnitude (i.e., scaled such that the signal energy was constant); in this way, each pattern vector is accorded equal importance when deriving the KLT basis functions.

Since the durations of the ST-T complexes vary (the final part of the ST-T complex is not always available due to the appearance of the next P-wave and QRS complex), the estimation of certain elements of the covariance matrix is problematic. Although one might extend the pattern vectors (by adding zero elements) so that all are of equal length, this procedure would tend to reduce the significance of non-zero elements in these positions when they are available, thereby lending an artifactual bias in favour of the initial elements. We prefer to address this issue by estimating each element of the covariance matrix using only those ST-T complexes for which the corresponding elements are available. This procedure avoids introducing artifacts of the window definition into the covariance matrix estimate; its consequence is that the final portions of the derived basis functions are derived from a smaller sample than the initial portions.

[Figure 1 about here.]

In Fig. 1 we plot the cumulative eigenvalue energy (CEE) *Fig.* 1

$$CEE(n) = 100\frac{\sum_{k=0}^{n}\lambda_k}{\sum_{k=0}^{N-1}\lambda_k} \quad (3)$$

as a function of the $KL_n$ order $n$, for the KLT basis functions derived using pattern vector set 1 (with cubic spline baseline correction, Fig. 1a) and for the KLT basis functions derived using set 2 (with correction *Fig.* 1a for heart rate, Fig. 1b). Note how the CEE for set 2 is higher than the CEE for set 1 for low values *Fig.* 1b of $n$, reflecting the reduction in waveform variability once the effects of heart rate are (at least in part) accounted for. This results in representing approximately 5% more energy by the first two HR corrected basis functions than by their uncorrected counterparts (Fig. 1). In the training set, the average HR is *Fig.* 1 quite low, as a result of our requirement of minimal baseline wander (generally accompanying low levels of physical activity and consequent low HR). This works to the disadvantage of the set 1 basis functions, since there is relatively little representation of ST-T complexes corresponding to high HR, with energy concentrated in the initial part of the window. The HR-corrected pattern vectors corresponding to ST-T complexes in high HR, however, closely resemble those in set 2, and are thus better represented by the low-order KLT coefficients of set 2 than those of set 1 (for an example, see section 2.2).

Although correction for HR produces an improvement in the quality of the KLT, we do not observe any improvement using high-pass or band-pass filtering (pattern vector sets 3, 4, 5, and 6). This result agrees with the supposition that the KLT is the most effective linear method for separating the signal from the noise, and that any other linear filter cannot produce further improvements. Cubic-spline correction of baseline variation produced slightly better results than high-pass filtering.

The first 14 KLT basis functions are displayed in Fig. 2 for the uncorrected set 1 (solid lines) and for the *Fig.* 2 corrected set 2 (dashed lines). It is apparent that the energy in the corrected set is concentrated at a later time than in the uncorrected set. Since most heart rates exceed 60 beats per minute, the correction applied to most ST-T complexes tends to stretch them (i.e., to move the concentration of energy toward the end of the window). The first basis function, and to a lesser extent the second one, represent the dominant low-frequency components of the ST-T complex concentrated in the first 400 ms after the QRS. The next few basis functions contain more high-frequency energy, and contain energy more evenly distributed across the entire complex. These functions represent components present in abnormally prolonged ST-T complexes and in U waves where present within the window. The remaining higher-order basis vectors shown in Fig. 2 contain almost exclusively high-frequency content related to noise in the training set. By inspection *Fig.* 2 of the basis vectors, we can predict that the first two KLT coefficients, $kl_0(i)$ and $kl_1(i)$, should be a good tool for detecting ischemic ST-T changes, since they contain virtually all of the low-frequency energy; we discuss this point further in section 3.2 below. Also, looking to the basis 0, it is apparent that it will mostly represent ST segment elevation waveforms (has a positive value at the ST segment) that will result

in positive $kl_0(i)$ values, on the contrary, basis 1 (has a negative value at the ST segment) will represent ST segment depressions waveforms resulting in positive $kl_1(i)$ values.

[Figure 2 about here.]

### 2.2 KLT representation of the ST-T complex

[Figure 3 about here.]

To illustrate the ability of the KLT to represent an arbitrary ST-T complex, we will analyze in this section the reconstruction of several real ST-T complexes. In Fig. 3 we present the reconstruction of three ST-T complexes with 3, 5 and 8 KLT coefficients, using both set 1 (uncorrected) and set 2 (HR-corrected) KLT basis functions. The first complex (Fig. 3a,b) includes a prominent U wave. Since high amplitude of U waves was unusual at the training set, a faithful reconstruction requires more than the first few KLT coefficients. The RR interval in this case is 1228 ms, implying only a small HR correction; we see, however (Fig. 3b) how this small shift to the left results in a markedly better reconstruction with the low order coefficients. At the right, the cumulative signal energy ($CE(n) = 100 \sum_{j=0}^{n} kl_j^2 / \sum_{k=0}^{N-1} STT^2(k)$) is shown for each reconstruction. Panels c and d of Fig. 3 show an ST-T complex during high HR (RR=440 ms). The signal energy is concentrated in the earliest part of the ST-T, and is poorly represented by the uncorrected KLT coefficients (Fig. 3c). The HR correction in this case shifts the ST-T complex to the right, producing a much better representation with the first three coefficients (Fig. 3d). This example shows the value of HR correction in cases where the HR is quite far from typical values. Finally, panels e and f of Fig. 3 present the reconstruction of a biphasic ST-T complex with RR=812 ms. Given that this shape is not dominant in the training set, more coefficients are required for an accurate reconstruction than in typical cases. The HR correction in this case is small, but a small improvement in the low-order reconstruction is still obtained. It always remains the question of how many coefficients are needed for an accurate reconstruction. For very rare wave-shapes (that always can occurs) it may be required a much larger number of KLT coefficients, but in our studies we did not found clinically significant wave-shapes that were not well overall reconstructed with the first 3 to 4 coefficients.

*Fig.* 3 *Fig.* 3a,b *Fig.* 3b *Fig.* 3 *Fig.* 3c *Fig.* 3d *Fig.* 3

## 3 Monitoring the $kl_n(i)$ series

In previous section we have described how to derive a KLT representation of a single ST-T complex. In clinical practice, the dynamic behaviour over time of ST-T morphology is even more important than the characteristics of an isolated complex. ST-T dynamics can be characterized by the study of KLT coefficient time series, $kl_n(i)$, using many of the techniques used in studies of HRV. We can assign to each beat mark

(QRS fiducial point) the KLT coefficients of its ST-T complex. In this way we will have as many (scalar) time series as there are KLT coefficients needed to represent the ST-T complex. The direct way to monitor $kl_n(i)$ is to obtain it from the inner product of the KLT basis with the pattern vectors of the ST-T complexes to be analyzed. These pattern vectors are obtained in the same manner as those in the training set (using cubic spline baseline removal, and HR correction if we are using the set 2 KLT). In this case, however, we do not normalize the energy of the ST-T complex pattern vectors, since we are interested in monitoring variations in energy as well as in morphology. We are not so restrictive as in the training set for rejecting beats, since now the obtained $kl_n$ will influence only the beat that represent and not affect the others as could happen if considered at the training set. The inner product is performed over the interval in which the ST-T complex is defined (not necessarily the entire window over which the basis function extends); this policy is equivalent to appending additional zero components to the pattern vector as needed to match its length to that of the basis function (see section 2.1).

Direct estimation in this way, however, results in a noisy $kl_n(i)$ time series. Noise is introduced into the $kl_n(i)$ time series from a variety of sources, including noise in the ST-T complexes not removed by the KLT, residual error in the KLT domain representation of the ST-T complexes, misestimation of the isoelectric level (because of noise in the PR interval, or QRS fiducial misestimation), residual baseline variations, and ectopic beats not rejected. Noise in the $kl_n(i)$ time series may be reduced using an adaptive filter that removes noise uncorrelated with the ST-T complex. This technique is useful for monitoring medium- to long-term variations in the ST-T complex, such as for detecting ischemic ST-T changes; on the other hand, when we are interested in beat to-beat variations (alternans), direct $kl_n(i)$ estimation is necessary.

### 3.1 The adaptive $kl_n(i)$ estimate

Adaptive estimation of quasi-periodic signals such as the ST-T complex permits reduction of noise uncorrelated with the signal, with attendant improvements in the ability to track subtle dynamic variations in these signals. This technique has been applied to analysis of ECG signals (Laguna et al., 1996a; Laguna et al., 1992) and evoked potentials (Thakor et al., 1993). It makes use of the recurring features of the signal and is based on the adaptive linear combiner (Widrow and Stearns, 1985).

[Figure 4 about here.]

In effect, the adaptive filter input signal (the *primary input*, $d_k$) consists of concatenated ST-T complexes only, with all intervening data removed. Short complexes are lengthened by appending zeroes as necessary, so that a new complex begins every $N$ samples. The adaptive system dynamically estimates the amount of each reference input present in the input signal. In (Laguna et al., 1996a) the reference inputs used for the estimation of the deterministic signal were the orthonormal Hermite functions; in (Laguna et al.,

1992) the reference inputs were unit impulses, and in (THAKOR ET AL., 1993) they were sine, cosine and Walsh functions. In the present study, the reference inputs are the KLT basis functions to be used to represent the ST-T complexes.

Figure 4 shows this process in schematic form. We define the beginning of each ST-T complex (85 ms following the QRS fiducial mark in each case) as the time of the *stimulus*. The N samples that follow the stimulus are assumed to be the sum of the signal of interest (a deterministic signal component, $s_k = STT_k$, correlated with the stimulus) and an uncorrelated noise component $n_k$. If the deterministic component is strictly periodic with a period of $N$ samples, then it satisfies $s_k = s_{k+N}$ for all $k$. *Fig.* 4

The reference inputs $KL_{j\ k}$ $(j = 0, ..., n-1)$ $(n \leq N)$ are formed by concatenating copies of the $j$th KLT basis function to be used to represent the ST-T complexes; thus $KL_{j\ k} = KL_{j\ k+N}$.

In the KLT vectorial space, $d_k$ may be expressed as the sum of all the KLT components and the uncorrelated noise:

$$d_k = \sum_{j=0}^{N-1} kl_j \, KL_{j\ k} + n_k \, . \tag{4}$$

The output of the adaptive filter, $y_k$, is the signal that we want to be an estimate of $s_k$, and $e_k$ is the error signal $e_k = s_k + n_k - y_k$ with

$$y_k = \sum_{j=0}^{n-1} w_{j\ k} \, KL_{j\ k} \tag{5}$$

If $\mathbf{KL}_k$ denotes the vector of reference inputs and $\mathbf{W}_k$ the weight vector

$$\mathbf{KL}_k = [KL_{0\ k}, KL_{1\ k}, ..., KL_{n-1\ k}]^T \qquad \mathbf{W}_k = [w_{0\ k}, w_{1\ k}, ..., w_{n-1\ k}]^T \tag{6}$$

then

$$y_k = \mathbf{KL}_k^T \, \mathbf{W}_k = \mathbf{W}_k^T \, \mathbf{KL}_k. \tag{7}$$

Minimizing the mean squared error $\xi = E[e_k^2]$ using any adaptive algorithm (WIDROW AND STEARNS, 1985), the weight vector converges to the optimal solution $\mathbf{W}^* = \mathbf{R}^{-1}\mathbf{P}$ (WIDROW AND STEARNS, 1985), where

$$\mathbf{R} = E[\mathbf{KL}_k \, \mathbf{KL}_k^T] \quad \text{and} \quad \mathbf{P} = E[d_k \, \mathbf{KL}_k] \tag{8}$$

In this case, given the orthonormality conditions of the base elements of KLT vectorial space and (by definition) the lack of correlation between the noise $n_k$ and the KLT basis $KL_{n\ k}$, $\mathbf{R}$ and $\mathbf{P}$ reduce to

$$\mathbf{R} = \frac{1}{N}\mathbf{I} \quad \text{and} \quad \mathbf{P} = \frac{1}{N}[kl_0, kl_1, ..., kl_{n-1}]^T \, , \tag{9}$$

and the optimal weight vector, $\mathbf{W}^*$, that minimizes the mean squared error, $\xi = E[e_k^2]$, is given by

$$\mathbf{W}^* = [kl_0, kl_1, ..., kl_{n-1}]^T \, . \tag{10}$$

This result means that each weight $w_i$ is an estimate of the $i$th KLT coefficient for $s_k$. Thus the weight vector is a characterization of the deterministic signal component, and the output signal $y_k$, in the optimum case, takes the value

$$y_k = \sum_{j=0}^{n-1} w_i^* \; KL_{j\;k} = \sum_{j=0}^{n-1} kl_j \; KL_{j\;k} \; , \tag{11}$$

i.e., the projection of $s_k$ onto the subspace spanned by $KL_{j\;k}$ $(i = 0, ..., n-1)$ with $n \leq N$. Thus $y_k$ is the $n$th-order KLT representation of $s_k$, and $y_k = s_k$ if $n = N$ (i.e., if all of the KLT components are included).

The minimum mean squared error, $\xi_{min}$, will be

$$\xi_{min} = E[d_k^2] - \mathbf{P}^T \mathbf{W}^* \; . \tag{12}$$

Given that the weight vector oscillates around this optimal value, $y_k$ is an unbiased estimate of $s_k$. The remaining noise due to the misadjustment $(M)$ depends upon the adaptive algorithm used to adjust the weight vector (Widrow and Stearns, 1985). The elements of the weight vector, evaluated at the end of each ST-T complex, are the adaptive estimates of the KLT coefficients of that complex. The quality of the $y_k$ estimation is thus directly related to the quality of the KLT estimation.

In this study, we have used the Least Mean Squares (LMS) algorithm (Widrow and Stearns, 1985)

$$\mathbf{W}_{k+1} = \mathbf{W}_k + 2\mu e_k \, \mathbf{KL}_k. \tag{13}$$

The condition that assures the convergence of the algorithm is (Feuer and Weinstein, 1985):

$$0 < \mu < \frac{1}{3 \; tr[\mathbf{R}]} = \frac{N}{3n} \; . \tag{14}$$

The time constant $(\tau_{mse})$ for the convergence of the MSE is:

$$\tau_{mse} = \frac{1}{4 \, \mu \lambda} = \frac{N}{4\mu} \; , \tag{15}$$

where $\lambda = \frac{1}{N}$ is the eigenvalue of the matrix $\mathbf{R}$ (all the eigenvalues are identical). $\tau_{mse}$ is expressed in sampling intervals. The gain constant, $\mu$, thus controls the stability and the speed of convergence. The estimate of the weight vector may be obtained within a single beat given an appropriate choice of $\mu$ that satisfies, $(\tau_{mse} < N)$ if necessary. Thus adaptive filtering may be used in principle even for tracking beat-by-beat ST-T variations.

To measure the excess of mean squared error we calculate the misadjustment (Widrow and Stearns, 1985)

$$M = \frac{Excess \; MSE}{\xi_{min}} \; , \tag{16}$$

which for the LMS algorithm can be approximated by (Widrow and Stearns, 1985):

$$\mathbf{M} \simeq \mu \; tr[\mathbf{R}] = \mu \frac{n}{N}. \tag{17}$$

The mean square error $\xi$ is

$$\xi = \xi_{min}(1+M) = \left(1+\frac{\mu\, n}{N}\right)\ \left(\frac{1}{N}\sum_{j=n}^{N-1} kl_j^2 + E[n_k^2]\right)\ . \tag{18}$$

The MSE thus depends on the noise power, the power in the ST-T complex not represented by the first $n$ $kl_n$ coefficients, and the gain constant, $\mu$. Note that the dependence on the KLT order $n$ is not strong, since an increase in $n$ value increases the $\left(1+\frac{\mu\, n}{N}\right)$ factor and decreases the $\sum_{j=n}^{N-1} kl_j^2$ factor. Thus, the optimum solution minimizes $n$ and maximizes $\sum_{j=0}^{n-1} kl_j^2$; this property is intrinsic to the KLT. Given that at the steady state the estimated signal $y_k$ is orthogonal to the error $e_k$ (Widrow and Stearns, 1985), the $Excess\, MSE$ is the excess of error power introduced in $y_k$, and the signal-to-noise ratio of this estimation, $SNR_y$, will be

$$SNR_y = \frac{\frac{1}{N}\sum_{j=0}^{n-1} kl_j^2}{\left(\frac{\mu\, n}{N}\right)\ \left(\frac{1}{N}\sum_{j=n}^{N-1} kl_j^2 + E[n_k^2]\right)}\ . \tag{19}$$

If we consider that the ST-T energy is strongly concentrated in the $n$ first coefficients, we can neglect the term $\sum_{j=n}^{N-1} kl_j^2$, obtaining

$$SNR_y = \frac{\frac{1}{N}\sum_{j=0}^{N-1} kl_j^2}{\left(\frac{\mu\, n}{N}\right)\ E[n_k^2]} \simeq SNR_d \frac{N}{\mu\, n}\ . \tag{20}$$

where $SNR_d$ is the SNR of the original signal. Comparison of this $SNR_y$ with that obtained from the direct estimation of $kl_n(i)$ will give the SNR improvement ($\triangle SNR$) achieved by the adaptive system. Direct $kl_n(i)$ estimation yields a signal-to-noise ratio, $SNR_y^{direct}$, that can be estimated if we assume the noise is white and that its PSD is uniformly distributed in the KLT domain:

$$SNR_y^{direct} = \frac{\frac{1}{N}\sum_{j=0}^{n-1} kl_j^2}{E[n_k^2]\frac{n}{N}} \simeq SNR_d \frac{N}{n}. \tag{21}$$

Thus the SNR improvement obtained using the adaptive filter is

$$\triangle SNR = \frac{SNR_y}{SNR_y^{direct}} = \frac{1}{\mu} \tag{22}$$

Thus we find that, for appropriately chosen values of $\mu$, the adaptive estimate of $kl_n(i)$ is cleaner than a $kl_n(i)$ time series obtained directly from the inner product. The choice of $\mu$ involves the typical trade-off between stability and rate of convergence, which limits the amount of improvement that can be obtained in practice, given the need to track changes occurring within a few beats in typical cases. When the interest of the estimation is in the ischemic changes that occur gradually from beat to beat the convergence restriction will be that it occurs in a reduced number of beats. Next section will consider the real case election.

### 3.2 Application to real signals with ischemic episodes

In this section we present the results of estimating and monitoring the $kl_n(i)$ values on several real ECG records. The parameters that we have selected for the adaptive estimate are $\mu = 0.1$, with $n = 4$ $kl_n(i)$ functions and $N = 150$. These values do not approach the convergence limit $\mu_{lim} = 12.5$, and give a time

constant $\tau_{mse} = \frac{N}{4\mu} = 375 = 2.5$ beats. This convergence time is reasonable for monitoring ischemic ST changes that typically occur over much longer intervals. The $\triangle SNR$ obtained in this case is $1/\mu = 10$ dB, representing a large improvement in the $kl_n(i)$ estimation.

The real signals are taken from the European ST-T database (TADDEI ET AL., 1992). This database contains records manually annotated by clinical experts who identified episodes of significant ST-T changes consistent with ischemia. The database was designed to provide a resource for the development and evaluation of automated ischemia detectors. All of the patient records in the database have been analyzed with our KLT technique, and its performance is illustrated by several selected cases chosen to illustrate the properties of the KLT technique.

[Figure 5 about here.]

To assist in the interpretation of the $kl$ coefficients we show in Fig. 5 the $kl_0$ time series from the ECG of a patient during Percutaneous Transluminal Coronary Angioplasty (PTCA). The ST-T complex shows marked morphological variations from inflation to post-inflation. Note that how during the first period (balloon inflation) the ST segment is positive as is $kl_0$. During the post-inflation period the ST-T complex inverts its amplitude and oscillates in magnitude. This is reflected in the $kl_0$ series as an oscillating negative value of the $kl_0$ coefficients. *Fig. 5*

[Figure 6 about here.]

Figure 6 illustrates $kl_n(i)$ time series, each two hours in length, for three ECG records from the European ST-T database. Fig. 6a compares the $kl_0(i)$ series of record e0103 for each of the two recorded ECG leads, estimated as the inner product between the ST-T complex and the first (uncorrected) KLT basis function. Fig. 6b shows the same series, obtained using the adaptive estimate with the parameters as given above, and showing a $\triangle SNR$ of about 10 dB compared with those of Fig. 6a. Note the simultaneous appearance of ischemic ST-T changes in both leads, which is repeated quasi-periodically. Note also the similarity of the temporal pattern of sequential ischemic episodes. The figure clearly shows eight ischemic episodes, corresponding to the eight peaks in the $kl_n(i)$ time series. Only five of these are marked in the database reference annotations, since three of these episodes (1th, 2th, and 7th) are below the standard thresholds for defining ischemic ST-T episodes. The technique we present allows these sub-threshold episodes to be identified unambiguously, and allows the long-term pattern of quasi-periodic ischemic changes to be observed more clearly than would be possible otherwise. Since the time series are initialized to zero, the time required for the adaptive algorithm to reach steady state (at the left edge of plots 6b, d, f) can be seen to be negligible in comparison with the evolution of the ischemic variations. *Fig. 6* *Fig. 6a* *Fig. 6b* *Fig. 6a*

Fig. 6c shows the $kl_0(i)$ (left) and $kl_1(i)$ (right) series of the ECG signal (only lead MLIII) of record e0105, and Fig. 6d shows their adaptively estimated counterparts. In this case, each of the seven peaks *Fig. 6c* *Fig. 6d*

corresponds to an ischemic ST-T episode marked in the database reference annotations. By study of two or more KLT coefficients in a single lead, we can easily monitor changes in ST-T morphology. Note how the ST segment elevation that corresponds to potential ischemia in the e0105 record, results in increased $kl_0(i)$ values and decreased (negative) $kl_1(i)$ values, as pointed out in section 2.1. Note again that the temporal pattern of each ischemic episode is quite constant.

Finally, in Fig. 6e the uncorrected and HR-corrected $kl_0(i)$ time series for the first ECG signal of record e0113 are shown, and Fig. 6f shows their adaptively estimated counterparts. As in the previous examples, the adaptive estimation of ST morphology tracks ischemic changes noted in the reference annotation files of the database. Note the slightly higher amplitude of the peaks in the HR-corrected series, showing that the first corrected $kl_n(i)$ basis function is better able to represent the ST-T complexes in this record than is the first uncorrected $kl_n(i)$ basis function. In Fig. 6f, we note that of the eight well-marked peaks, seven correspond to ischemic episodes annotated in the database, but one other (the second) was not so annotated in the database, although its presence is quite clear from inspection of the $kl_n(i)$ series.

*Fig.* 6e

*Fig.* 6f

*Fig.* 6f

In the examples presented in Fig. 6 it can be seen that both traces (adaptive and inner product estimated) reflect the ST-T changes. However when the changes are not so clearly defined (first salvo in a) b), last in e) , f)) the adaptive estimation is more suited. In addition when considering automatic ischemia detection, the influence of noise decreases sensitivity and specificity of the inner product with respect to those of adaptive estimate.

*Fig.* 6

Analyzing the entire European ST-T Database (90 records) we found that roughly 20% of the records demonstrated the quasi-periodic salvos of ST-T changes shown in Fig. 6. In most records containing multiple ST-T variation episodes, we noted similarity in the temporal structure of their $kl_n(i)$ time series, suggesting a similar pathophysiologic mechanism. It is clear that the KLT technique detects and locates transient ST-T variations. Subsequent detailed analysis of the record and/or collateral clinical information should be used to determine whether the ST-T variations are actually associated with ischemic episodes.

*Fig.* 6

This technique has been used to design an automatic ischemia detector (Gracía, 1998) making use of the first four *kl* series. The automatic detector can be configured to detect either ST segment, T wave or ST-T complex episodes (for the detector validation we used the manual annotations in ST segment and T wave from the European ST-T database and the OR combination of ST and T episodes for the ST-T complex (Taddei et al., 1992)). The preliminary results obtained in terms of sensitivity (S) and positive predictivity (+P) are S=81% and +P=80%, when detecting ST episodes. This shows a very good performance of the technique which can help clinicians in ischemic episodes detection in Holter ECGs and may be useful for alarms design in coronary care units.

### 3.3 $kl_n(i)$ series compared to $qt(i)$ series

Repolarization is reflected in both the shape of the ST-T waveform, and also in the duration of the QT interval. We compared the $kl_n(i)$ time series with the $qt(i)$ time series using the techniques for QT estimation described elsewhere (Laguna et al., 1994). An example from record e0103 is shown in Fig. 7. In this case the ischemic episodes are clearly manifested in the $kl_n(i)$ time series. The $qt(i)$ time series time series taken from lead III (but not that taken from lead V4) shows transient increases in QT interval during the first four ischemic episodes (but not the last three). The QT variations persisted when corrected for heart rate using Bazett's formula.

Figure 8 shows that the transient QT prolongation accompanies ischemic ST-T episodes (Fig. 8c), and becomes even more prominent when heart rate is corrected (Fig. 8d).

[Figure 7 about here.]

[Figure 8 about here.]

Analyzing the entire European ST-T Database (90 records) we found that roughly 50% of ischemic records showed QT variations in at least one lead associated with the ischemic episodes.

### 3.4 $kl_n(i)$ series compared to $st(i)$ series

To show the differences between conventional ST level monitoring and the $kl$ series monitoring we created ST level trend plots for several records and compared them to corresponding $kl$ time series. The weighted averaging method was used to measure the ST segment deviations. This method is especially useful when the beat-to-beat noise level changes. ST segments were selected from averaged ECG complexes. To assure convergence properties similar to those of the KLT estimation method previously described, only three beats were included in each sub-ensemble average. Also only normal beats surrounded by normal beats were included to avoid artifacts. Each beat was added into the average with a weighting factor inversely proportional to its noise content. The weighted average (Zhong and Lu, 1991) is given by:

$$\bar{x}(t) = \sum_{i=1}^{N_{beat}} w_i x_i(t) \tag{23}$$

where $N_{beat}$ is the number of beats to be averaged, $x_i$ is the $ith$ beat, and $w_i$ is the weight applied to that beat. For simple signal averaging $w_i = 1/N_{beat}$, ie, each beat has an equal weight. The weighting factor is

$$w_i = \left(\frac{1}{\sigma_i^2}\right)\left(\frac{1}{\sum_{j=1}^{N_{beat}} \frac{1}{\sigma_j^2}}\right) \tag{24}$$

where $\sigma_i$ is the noise power of the $ith$ beat. Once each three-beat average had been constructed, the ST level was measured by taking the mean value in a 10 ms interval centered 60 ms from the end of the QRS.

[Figure 9 about here.]

In Fig. 9a we show the $kl_0$ series of record e0129 (two leads) and in 9b the corresponding ST level series for each lead. Note the significant enhancement of the ST episodes by the KLT method, especially in lead V3. Figure 10 shows similar plots for record e0103, and again the superiority of the $kl$ trend plots is clear. From these examples and others throughout the ESC ST-T database, we confirmed our expectation that the KLT technique is much more robust and sensitive than the single ST level measure.

[Figure 10 about here.]

### 3.5 ST-T Alternans detection from the $kl_n(i)$ series

The KLT can also be used to detect alternans in the ST-T complex. Alternans may be an index of the risk of SCD (Clancy et al., 1991; Rosenbaum et al., 1994). We calculate a spectrum from the series of KLT coefficients, with the independent variable being the beat number. The spectrum obtained in this way is a beat spectrum (DeBoer et al., 1984) rather than a frequency spectrum; the units corresponding to frequency are cycles per beat ($beat^{-1} = b^{-1}$). This spectrum is best suited for study of alternans, since we are interested in beat periodicities rather than the time periodicities that require study of frequency spectra.

[Figure 11 about here.]

Figure 11 illustrates the detection of subtle alternans in record e0105 of the European ST-T Database using the $kl_n(i)$ series and its beat spectrum. This record presents alternans in association with the ST-T variation (potentially ischemic) episodes shown in Fig. 6. Fig. 11a shows beat-to-beat alternation of ST-T morphology during the first ST-T variation episode. Fig. 11b shows the $kl_0(i)$ series calculated directly (at left) and its beat spectrum (at right). The clear peak at 0.5 $b^{-1}$ represents the periodic beat-to-beat ST-T shape variations, visible in the time series as a high-frequency, high-amplitude modulation near the middle of the 15-minute series. In addition, the beat spectrum reveals the appearance of a 0.25 $b^{-1}$ peak associated with a period 4 variation in ST-T morphology, also observable in Fig. 11a. There is another peak at 0.0 $b^{-1}$ and its harmonic at 1.0 $b^{-1}$ that represent a DC component over the entire $kl_n(i)$ series. This comes from the overall $kl_n(i)$ variation due to the underlying ischemic evolution. Fig. 11c,d show another episode of alternans, occurring during the sixth ST-T variation episode of the record (see Fig. 6c,d) . In this episode, both period 2 and period 4 alternans are even more marked than in the first example. Although the alternans may be detected even when using adaptive $kl_n(i)$ estimates (Fig. 11e), the resulting attenuation of short-term variation makes it clear that the directly estimated $kl_n(i)$ series is better-suited for this purpose. Figure 11f (left) shows the HR spectrum, obtained using a technique for

*Fig.* 11
*Fig.* 6
*Fig.* 11
*Fig.* 11b
*Fig.* 11
*Fig.* 6

power spectral density estimation of irregularly sampled signals (Laguna et al., 1998); this spectrum confirms that the alternans is not an artifact of an underlying HR modulation. Figure 11f (right) shows the $kl_n(i)$ frequency spectrum, estimated using the same technique; the alternans is less apparent in this frequency spectrum than in the beat spectra, as a result of the change in HR that makes the alternans not strictly time periodic. The beat spectrum (Fig. 11d, right) of the $kl_n(i)$ is thus much more appropriate for alternans detection than the time spectrum (Fig. 11f, right). Finally figs. 11g,h show this analysis during a non-ischemic period of the same record. In this case, the beat-to-beat alternans has almost disappeared, but the period 4 alternans remains apparent. By study of the entire record, we can observe that the period 2 alternans appears in association with the ST-T variation episodes, usually in the later portions of each episode, but disappears rapidly during recovery. The period 4 alternans is also associated with the ST-T varying episodes, but persists after recovery. It seems that period 4 alternans is more prominent in the non-ischemic (Fig. 11h) than during ischemic periods (Fig. 11d). This happens because the total power is normalized to unity, and then when the period 2 disappears most of the relevant energy is at period 4. The interpretation should be done in relative terms rather than absolute.

Based on this beatquency spectrum and KLT series we developed an alternans detector (Laguna et al., 1996b) that detects alternans representing around 60 $\mu$V amplitude variations of the ST-T complex. A detailed analysis of the European ST-T database has shown that about 5% of ischemic episodes present alternans associated with them and also more than 50% of the alternans present in the recordings are associated with the ischemic episodes (Laguna et al., 1996b). This corroborates previous clinical works that highly relate the alternans phenomena with the ischemia. This detector can be used as a new index when analyzing Holter ECG recordings to prevent ventricular arrythmias.

# 4 Discousion and Conclusions

In this work we have presented a KLT technique for studying the repolarization period of the heart throughout the ST-T complex of the ECG signal. We have developed a KLT training set of ST-T complexes, containing a broad range of morphologies, to obtain the KLT basis vectors. We have shown that this representation permits about 90% of the signal energy to be represented by the first 4 $kl_n(i)$ coefficients. We have shown that heart rate correction of the ST-T complex using Bazett's formula improves the performance of the KLT, whereas neither linear high-pass nor linear bandpass filtering has any beneficial effect. The KLT has been used to detect ST-T shape variations, with results demonstrating its sensitivity for detecting ST variations (potentially related to ischemic events). We have described an adaptive filter, based on the adaptive linear combiner with the LMS algorithm, for improving the signal-to-noise ratio of a time series of KLT coefficients. The adaptive estimation system delivers an improvement of about 10 dB for a practical choice of parameters for monitoring ischemic ST-T changes. The direct estimates of the

KLT coefficient time series, and beat spectra derived from them, have been shown to be well-suited for study of ST-T alternans.

In demonstrating the application of these techniques to analysis of the entire European ST-T Database, we have shown that about 20% of the records reveal a quasi-periodic pattern of ischemic ST-T episodes, and another 20% exhibit repetitive but not clearly periodic patterns of ST-T change episodes. These observations are drawn from information coming from the entire ST-T complex; it would be difficult if not impossible to reach similar conclusions with confidence using classical differential measurements of ventricular repolarization such as measurements of ST level or QT interval. The salvo patterns of ischemia suggest an oscillatory or periodic instability of the coronary blood supply, perhaps due to cyclic vasospasm. More study of the phenomenon is warranted, since the temporal patterns of ischemia may guide therapeutic interventions. Preliminary results on automatic ischemia detection using 4 $kl$ coefficents give a sensitivity of 81% and a positive predictivity of 80% at the European ST-T database. Finally, we have observed alternans of periods 2 and 4 in association with ischemic episodes, with different responses to recovery. Period 4 alternans and the association of alternans with ST-T changes (ischemia) have not been previously reported; the techniques we describe make the study of these phenomena possible. However a complementary analysis of the respiration will be required to establish if the period 4 alternans are a results of the respiration rate coupled with HR or a intrinsic period 4 alternans. At complete analysis at the European ST-T database gives that 5% of the ischemic episodes present period 2 alternans associated with them.

The KLT technique can be used for long-term tracking of ST-T variations, and may open the door for developing improved automatic detectors of transient ST-T changes.

## References


Akselrod, S., Norymberg, M., Peled, I., Karabelnik, E., and Green, M. S. (1987). Computerized analysis of ST segment changes in ambulatory electrocardiograms. *Med. Biol. Eng. Comput.*, 25:513–519.

Bazett, H. C. (1920). An analysis of the time relation of electrocardiograms. *Heart*, 7:353–370.

Berbari, E. and Lazzara, R. (1988). An introduction to high-resolution ECG recordings of cardiac late potentials. *Arch. Intern. Med.*, 148:1859–1863.

Breithardt, G., Cain, M. E., El-Sherif, N., Flowers, N., Hombach, V., Janse, M., Simson, M., and Steinbeck, G. (1991). Standards for analysis of ventricular late potentials using high resolution or signal-averaged electrocardiography. *J. Am. Coll. Cardiol.*, 17:999–1006.

Clancy, E. A., Smith, J. M., and Cohen, R. J. (1991). A simple electrical-mechanical model of the heart applied to the study of electrical-mechanical alternans. *IEEE Trans. on Biomed. Eng.*, 38(6):551–560.

DeBoer, R. W., Karemaker, J. M., and Strackee, J. (1984). Comparative spectra of series of point element particularly for heart rate variability data. *IEEE Trans. on Biomed. Eng.*, 31:384–387.

Feuer, A. and Weinstein, E. (1985). Convergence analysis of LMS filters with uncorrelated Gaussian data. *IEEE Trans. Acoust., Speech, Signal Processing*, 33:222–230.

Gallino, A., Chierchia, S., Smith, G., Croom, M., Morgan, M., Marchesi, C., and Maseri, A. (1984). Computer system for analysis of ST segment changes on 24 hour Holter monitor tapes: Comparison with other available systems. *JACC*, 4(2):245–252.

Gracía, J. (1998). *Sistema de Monitorización y Detección de Isquemia Basado en la Transformada de Karhunen-Loève aplicada sobre el ECG*. PhD thesis, Universidad de Zaragoza, Zaragoza. In Spanish.

Haddad, R. A. and Parsons, T. W. (1991). *Digital Signal Processing. Theory Applications and Hardware*. Computer Science Press, New York.

Jager, F. J., Mark, R. G., Moody, G. B., and Divjak, S. (1992). Analysis of transient ST segment changes during ambulatory monitoring using the Karhunen-Loève transform. In *Computers in Cardiology*, pages 691 – 694. IEEE Computer Society Press.

Klieger, R. E., Miller, J. P., Bigger, J. T., and Moss, A. M. (1984). Heart rate variability: A variable predicting mortality following acute myocardial infarction. *J. Coll. Cardiol.*, 3:2.

Laguna, P., Jané, R., and Caminal, P. (1994). Automatic detection of wave boundaries in multilead ECG signals: Validation with the CSE database. *Comput. Biomed. Resear.*, 27(1):45–60.

Laguna, P., Jané, R., Meste, O., Poon, P. W., Caminal, P., Rix, H., , and Thakor, N. V. (1992). Adaptive filter for event-related bioelectric signals using an impulse correlated reference input: Comparison with signal averaging techniques. *IEEE Trans. Biomed. Eng.*, 39(10):1032–1044.

Laguna, P., Jané, R., Olmos, S., Thakor, N. V., Rix, H., and Caminal, P. (1996a). Adaptive estimation of QRS complex by the Hermite model for classification and ectopic beat detection. *Medical and Biological Engineering and Computing*, 34:58–68.

Laguna, P., Mark, R., Goldberger, A., and Moody, G. (1997). A database for evaluation of algorithms for measurement of QT and other waveform intervals in the ECG. In *Computers in Cardiology*. IEEE Computer Society Press.

Laguna, P., Moody, G. B., and Mark, R. (1998). Power spectral density of unevenly sampled data by least-square analysis: Performance and application to heart rate signals. *IEEE Trans. on Signal Processing*, 45(6):698–715.

Laguna, P., Ruiz, M., Moody, G. B., and Mark, R. G. (1996b). Repolarization alternans detection using the KL transform and the beatquency spectrum. In *Computers in Cardiology*, pages 673–676. IEEE Computer Society Press.

Lynn, P. A. (1977). Online digital filters for biological signals: Some fast designs for a small computer. *Med. Biol. Eng. Comput.*, 15:534–540.

Merri, M., Alberti, M., and Moss, A. J. (1993). Dynamic analysis of ventricular repolarization duration from 24-hour Holter recordings. *IEEE Trans. on Biomed. Eng.*, 40(12):1219–1225.

Meyer, C. R. and Keiser, H. N. (1977). Electrocardiogram baseline noise estimation and removal using cubic splines and state-space computation techniques. *Computers and Biomedical Research*, 10:459–470.

Moody, G. B. and Mark, R. G. (1982). Development and evaluation of a 2-lead ECG analysis program. In *Computers in Cardiology*, pages 39–44. IEEE Computer Society Press.

Moody, G. B. and Mark, R. G. (1990a). The MIT-BIH arrhythmia database on CD-ROM and software for use with it. In *Computers in Cardiology*, pages 185–188. IEEE Computer Society Press.

Moody, G. B. and Mark, R. G. (1990b). QRS morphology representation and noise estimation using the Karhunen-Loève transform. In *Computers in Cardiology*, pages 269–272. IEEE Computer Society Press.

Myers, G., Martin, G., Magid, N., Barnett, P., Schaad, J., Weiss, J., Lesch, M., and Singer, D. H. (1986). Power spectral analysis of heart rate variability in sudden cardiac death: Comparison to other methods. *IEEE Trans. Biomed. Eng.*, 33(12):1149–1156.

Puddu, P. E. and Bourassa, M. G. (1986). Prediction of sudden death from QTc interval prolongation in patients with chronic ischemic disease. *J. Electrocardiology*, 19(3):203–212.

Rosenbaum, D. S., Jackson, L. E., Smith, J. M., Garan, H., Ruskin, J. N., and Cohen, R. J. (1994). Electrical alternans and vulnerability to ventricular arrhythmias. *The New England Journal of Medicine*, 330(4):235–241.

Speranza, G., Nollo, G., Ravelli, F., and Antolini, R. (1993). Beat-to beat measurement and analysis of the R-T interval in 24 h ECG Holter recordings. *Med. Biol. Eng. Comput.*, 31(5):487–494.

Taddei, A., Distante, G., Emdin, M., Pisani, P., Moody, G. B., Zeelenberg, C., and Marchesi, C. (1992). The European ST-T database: standards for evaluating systems for the analysis of ST-T changes in ambulatory electrocardigraphy. *European Heart Journal*, 13:1164–1172.

Thakor, N. V., Guo, X., Vaz, C. A., Laguna, P., Jané, R., Caminal, P., Rix, H., and Hanley, D. (1993). Orthonormal (Fourier and Walsh) models of time-varying evoked potentials in neurological injury. *IEEE Trans. Biomed. Eng.*, 40(3):213–221.

Thakor, N. V., Webster, J. G., and Tompkins, W. J. (1984). Estimation of QRS complex power spectrum for design of a QRS filter. *IEEE Trans. Biomed. Eng.*, 31(11):702–706.

Widrow, B. and Stearns, S. D. (1985). *Adaptive Signal Processing.* Prentice-Hall, Englewood Cliffs, New Jersey.

Zhong, J. and Lu, W. (1991). On two weighted signal averaging methods and their application to the surface detection of cardiac micropotentials. *Comput. Biomed. Res.*, 24:332–343.

# List of Figures

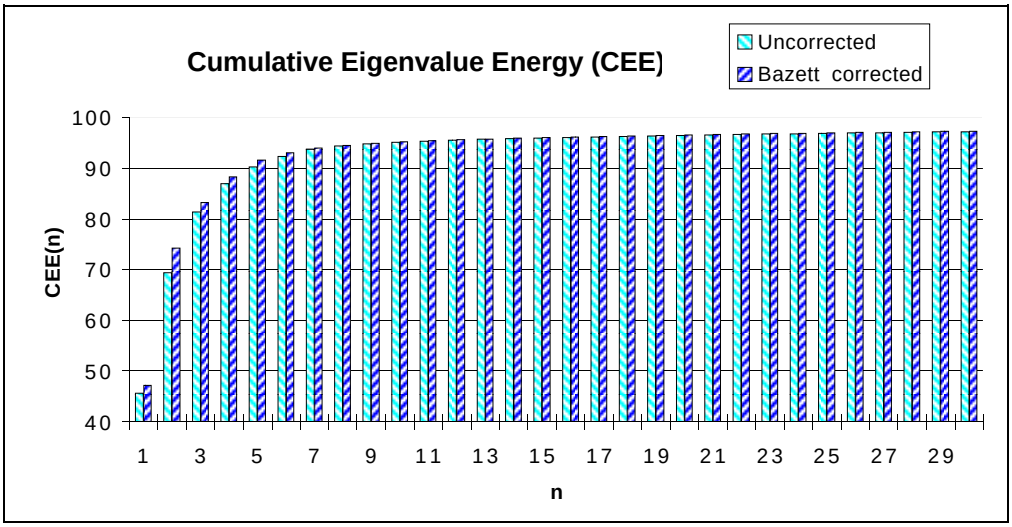


Figure 1: *Cumulative eigenvalue energy* $CEE(n) = 100 \sum_{k=0}^{n} \lambda_k / \sum_{k=0}^{N-1} \lambda_k$ *as a function of the sorted eigenvalue order* $n$. $N = 150$ *is the total number of eigenvalues* $\lambda_k$. *Light bars show results obtained using pattern vector set 1 (baselines corrected using cubic splines), and dark bars show results obtained using set 2 (with correction for heart rate).*

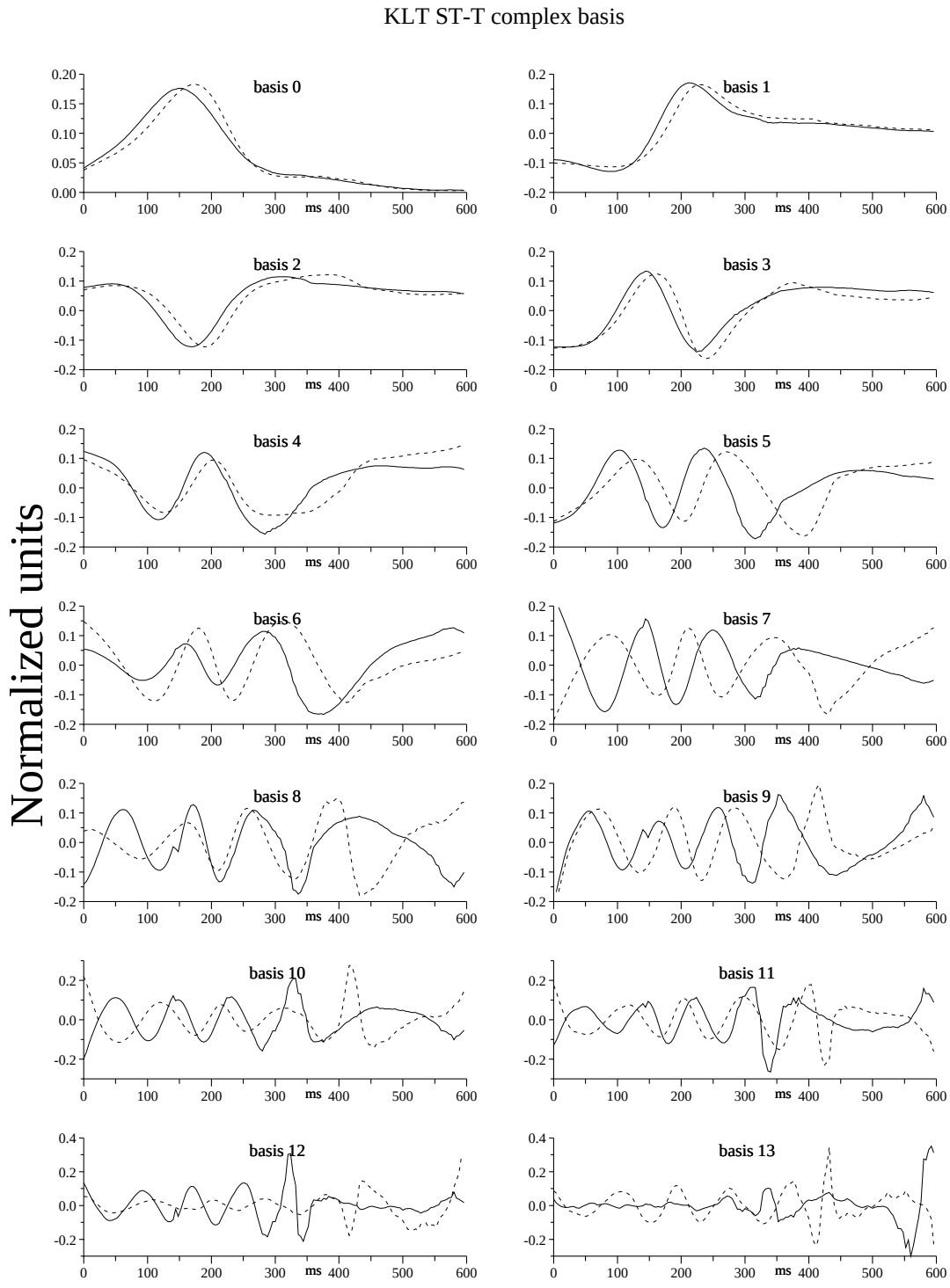


Figure 2: *KLT basis functions. The solid lines show functions derived from set 1 (without HR correction), while the dashed lines show functions derived from set 2 (with HR correction). The units of vertical axis are normalized (not mV) since the basis need to be orthonormal, and then they have been multiplied by a normalizing factor.*

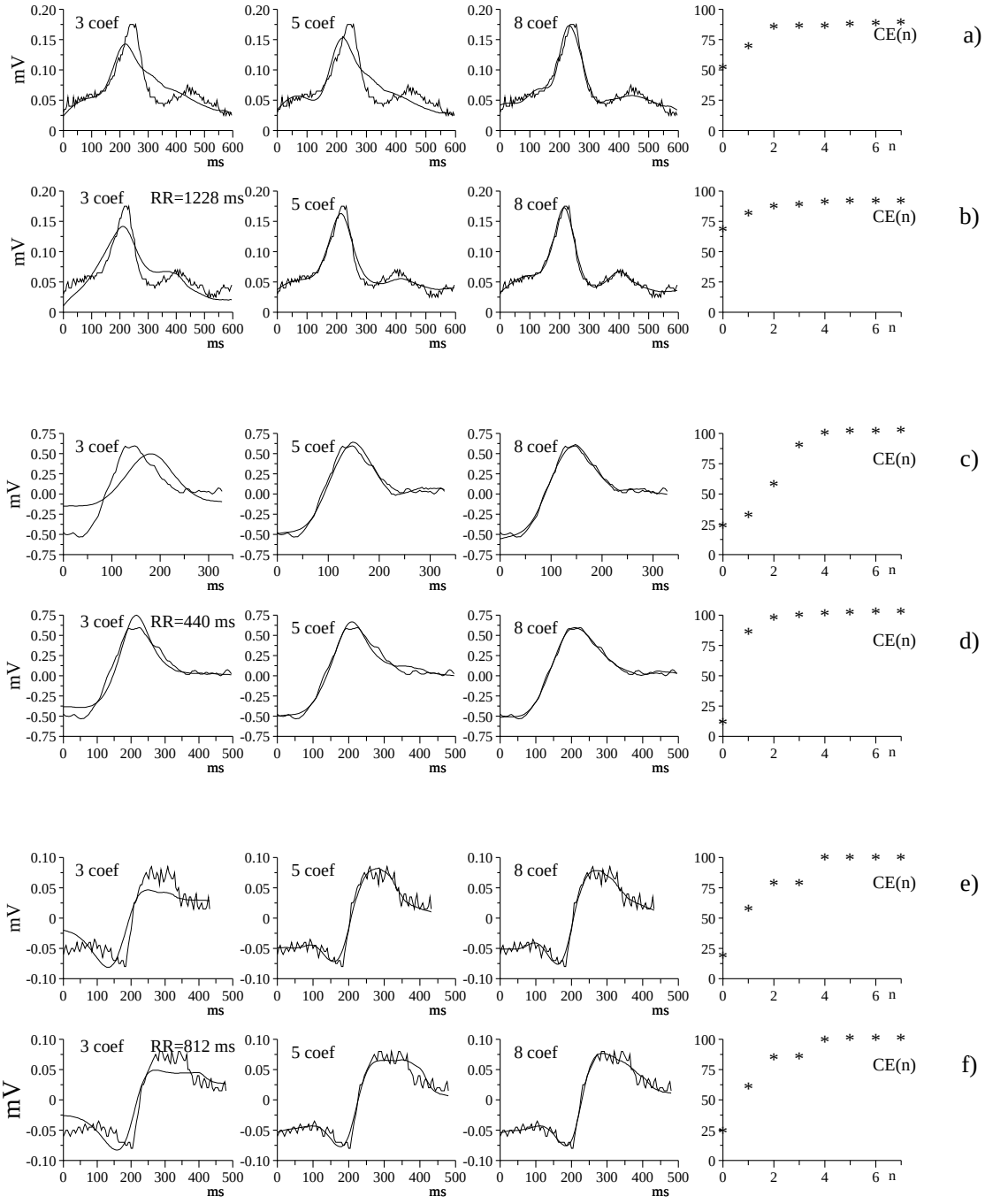


Figure 3: *Reconstruction of three ST-T complexes with the KLT. Panel (a) shows an ST-T complex with a U wave and its reconstruction based on 3, 5 and 8 KLT coefficients, together with the cumulative energy (CE(n)) as a function of the $kl_n(i)$ order (n), plotted at the right. In panel (a), the uncorrected (set 1) KLT has been used; panel (b) shows the same ST-T complex, reconstructed using the HR-corrected (set 2) KLT. Panels (c) and (d), and panels (e) and (f), show similar reconstructions for two other two ST-T complexes; see the text for descriptions.*

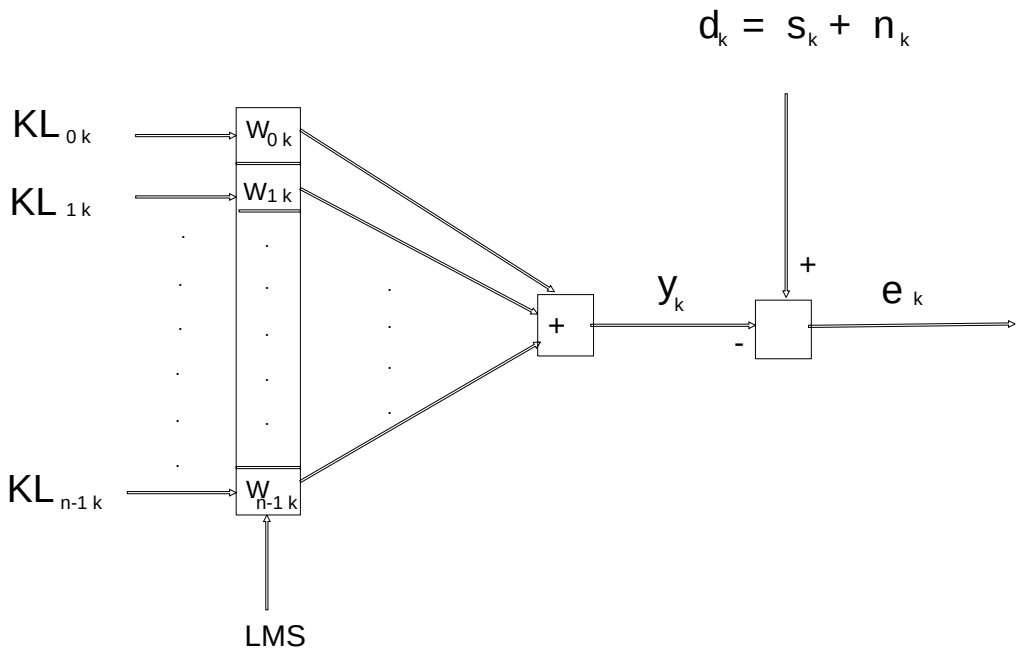


Figure 4: *Adaptive estimation system for the* $kl_n(i)$.

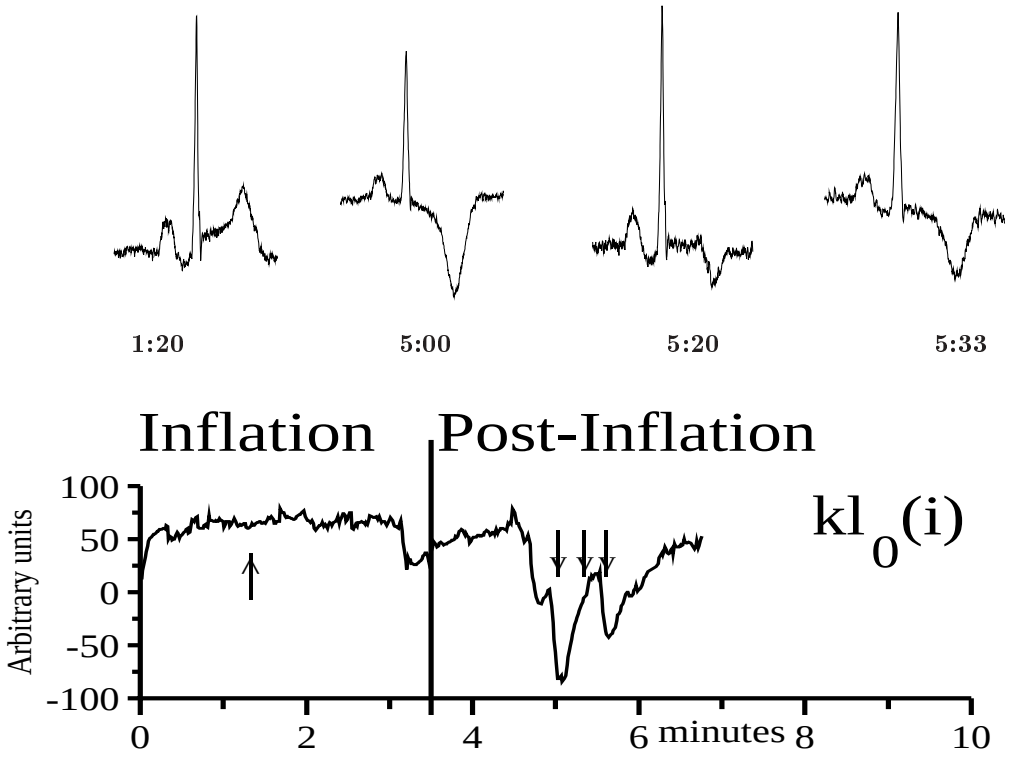


Figure 5: *Example of the time series of the first kl coefficient, $kl_0$, from a patient with large ST-T variations during PTCA. Four sample beats are shown at the top of the figure corresponding to the times indicated by the arrows on the $kl_0(i)$ series. Note how during the balloon inflation period the ST-T complex is positive, corresponding to positive $kl_0$ values. After deflation of the balloon, the ST-T complex inverts its polarity and oscillates in magnitude.This is reflected in the $kl_0$ time series as a negative oscillating value.*

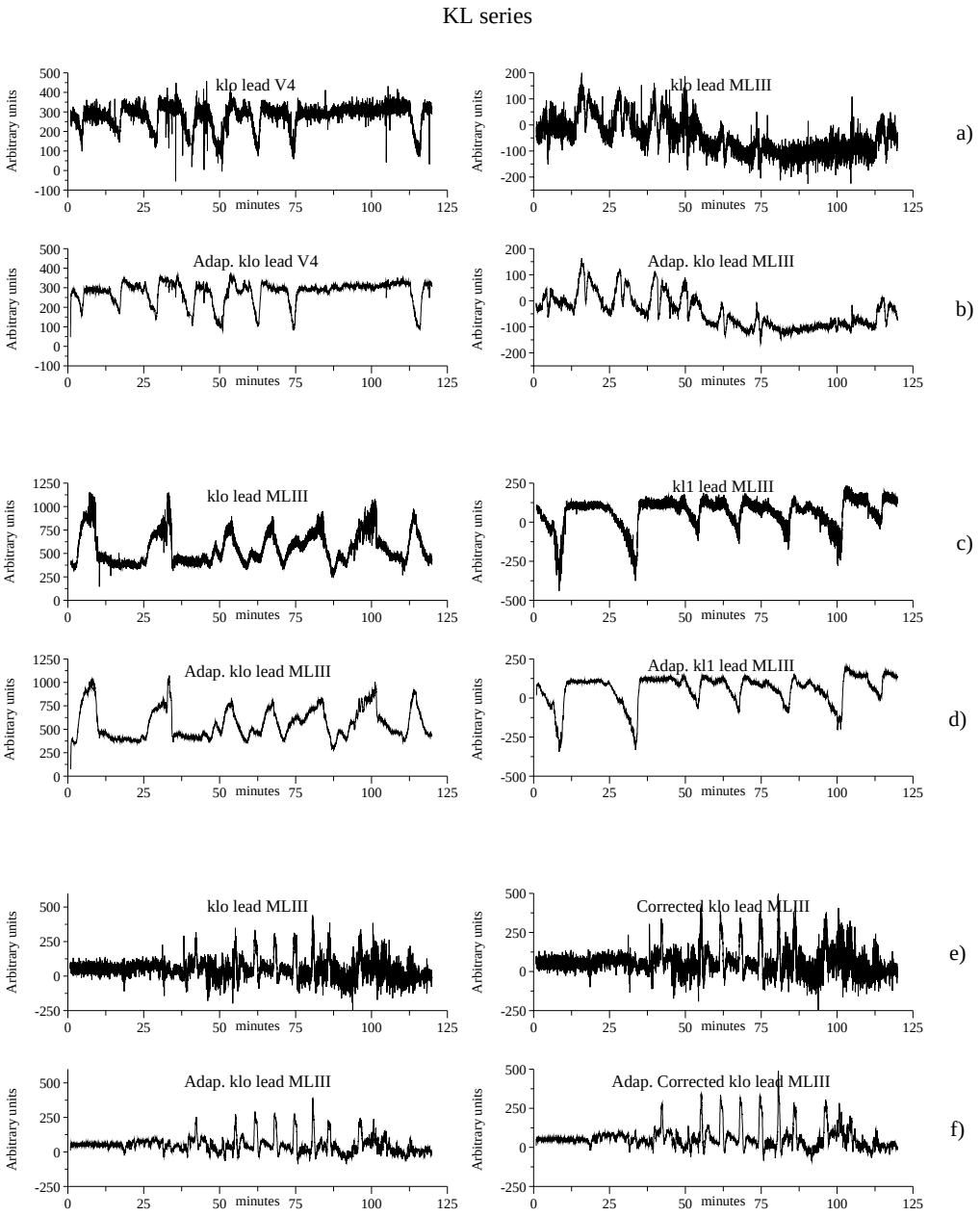


Figure 6: *$kl_n(i)$ plots for three records of the European ST-T Database. Panels (a) and (b) present $kl_0(i)$ time series of record e0103 estimated directly from the inner product (a), and with the adaptive estimate (b); those on the left correspond to the first lead (V4), and those on the right to the second lead (MLIII). Panels (c) and (d) show the $kl_0(i)$ time series for record e0105 on the left, and the $kl_1(i)$ time series for the same lead (MLIII) on the right. Panels (e) and (f) illustrate the uncorrected $kl_0(i)$ time series for record e0113 on the left, and the corresponding HR-corrected $kl_0(i)$ time series on the right for the same lead (MLIII). The temporal axes reflect the time instant at which the beat, corresponding to the kl value, appears.*

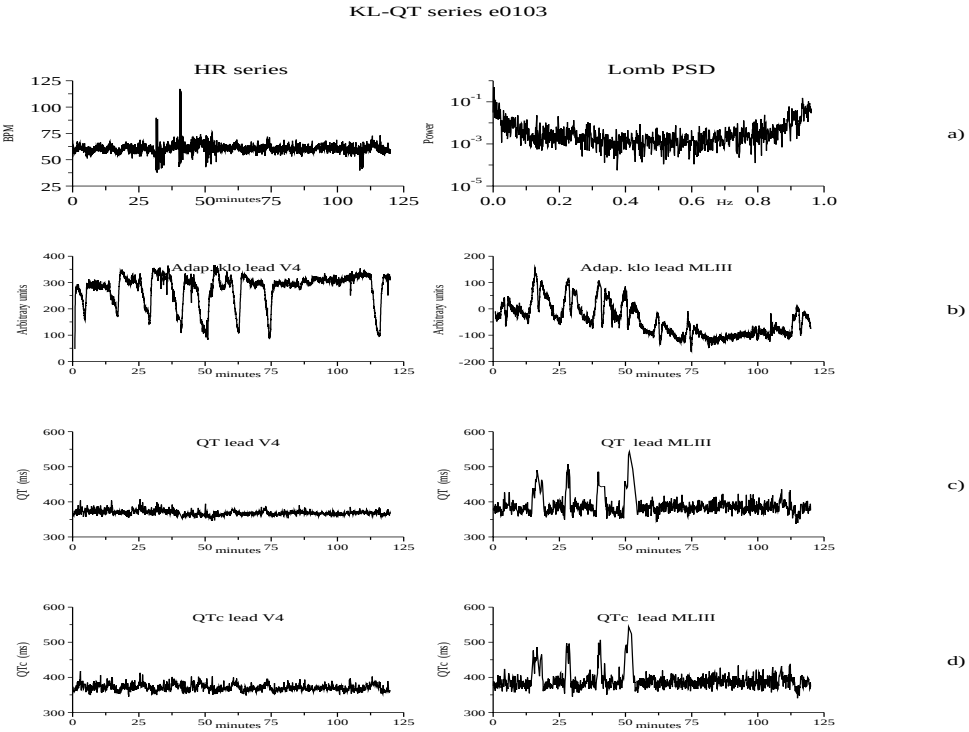


Figure 7: *kl and qt plots for record e0103 of the European ST-T Database. Panel (a) shows the heart rate (left) and its power spectrum density (right) estimated with the Lomb spectrum[32] (only frequencies up to the inverse mean heart period are meaningful), (b) presents the $kl_0$ time series estimated with the adaptive filter for lead V4 (left) and lead MLIII (right), (c) shows the qt series for both leads estimate as the mean after rejecting the maximum and minimum values in five beat sets. (d) show the Bazett's corrected qt series.*

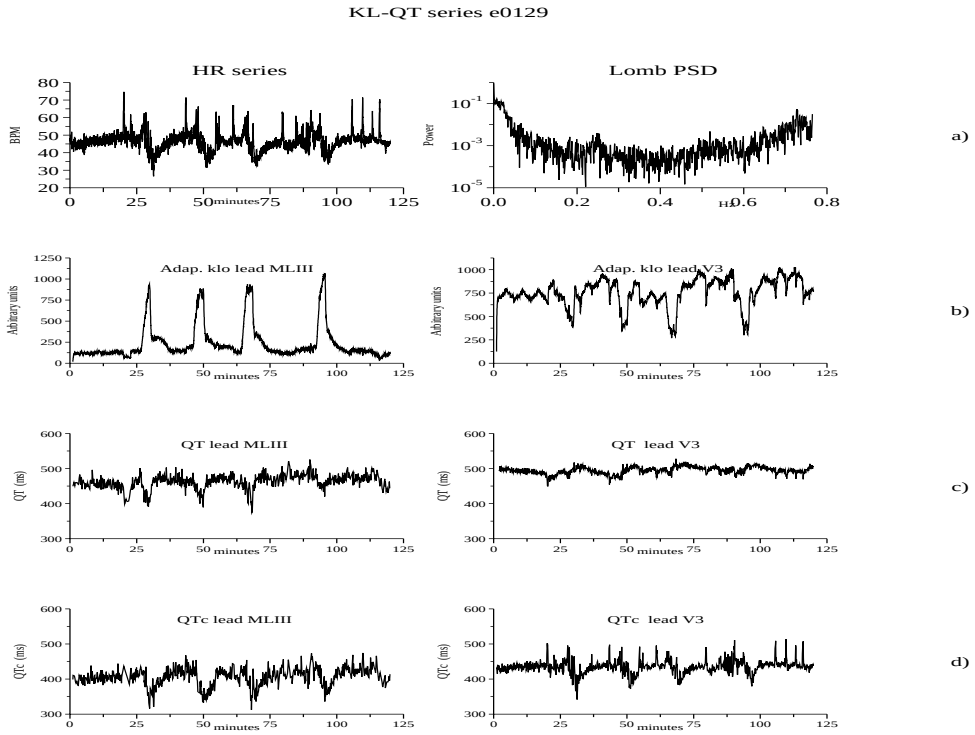


Figure 8: *$kl_n(i)$ and $qt(i)$ plots for record e0129 of the European ST-T Database. Panel (a) shows the heart rate (left) and its power spectrum density (right) estimated with the Lomb spectrum[32] (only frequencies up to the inverse mean heart period are meaningful), (b) shows the $kl_0(i)$ time series estimated with the adaptive filter for lead MLIII (left) and lead V3 (right), (c) shows the $qt(i)$ series for both leads estimated as the mean after rejecting the maximum and minimum values in five beat sets. (d) show the Bazett's corrected $qt(i)$ series.*

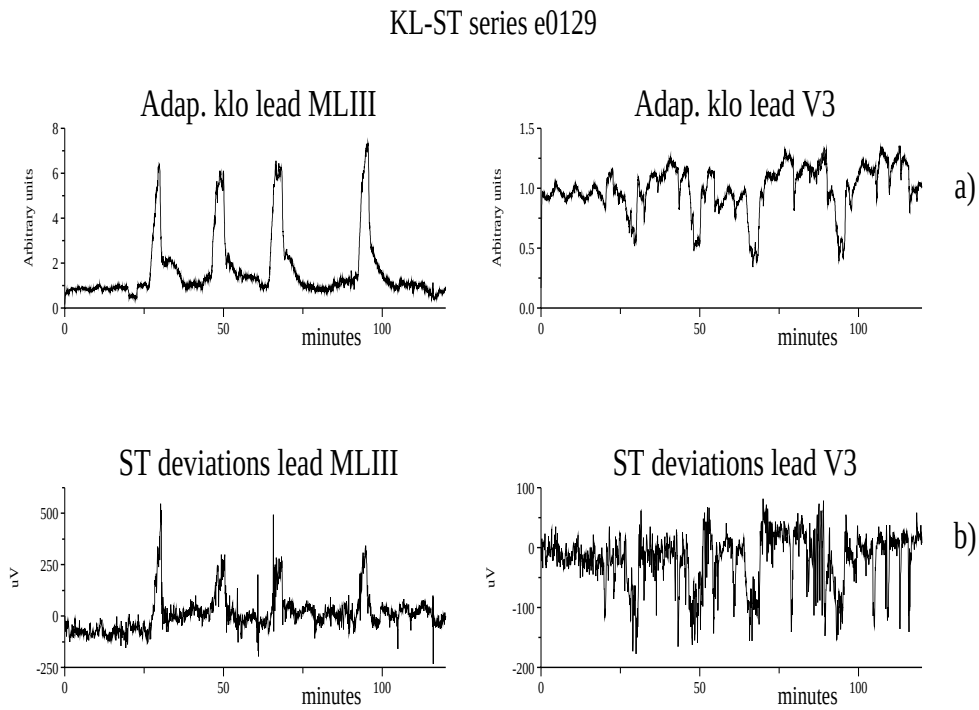


Figure 9: *$kl_n(i)$ and $st(i)$ plots for record e0129 of the European ST-T Database. Panel (a) shows the $kl_0(i)$ time series estimated with the adaptive filter for lead MLIII (left) and lead V3 (right), (b) presents the $st(i)$ series for both leads estimated as described in the text.*

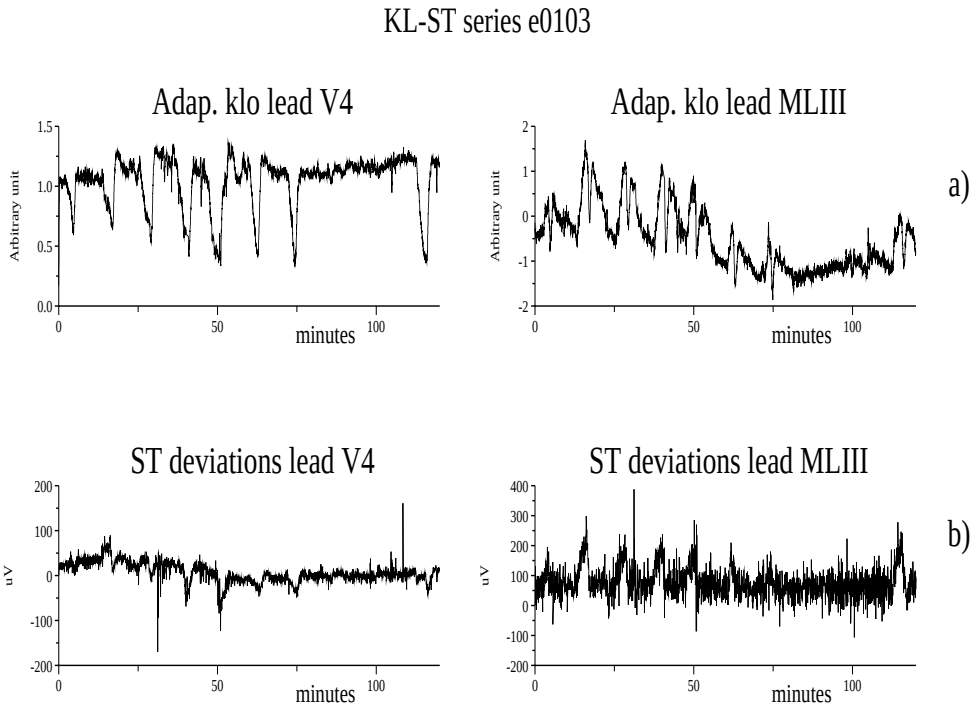


Figure 10: *$kl_n(i)$ and $st(i)$ plots for record e0103 of the European ST-T Database. Panel (a) shows the $kl_0(i)$ time series estimated with the adaptive filter for lead V4 (left) and lead MLIII (right), (b) presents the $st(i)$ series for both leads estimated as described in the text.*

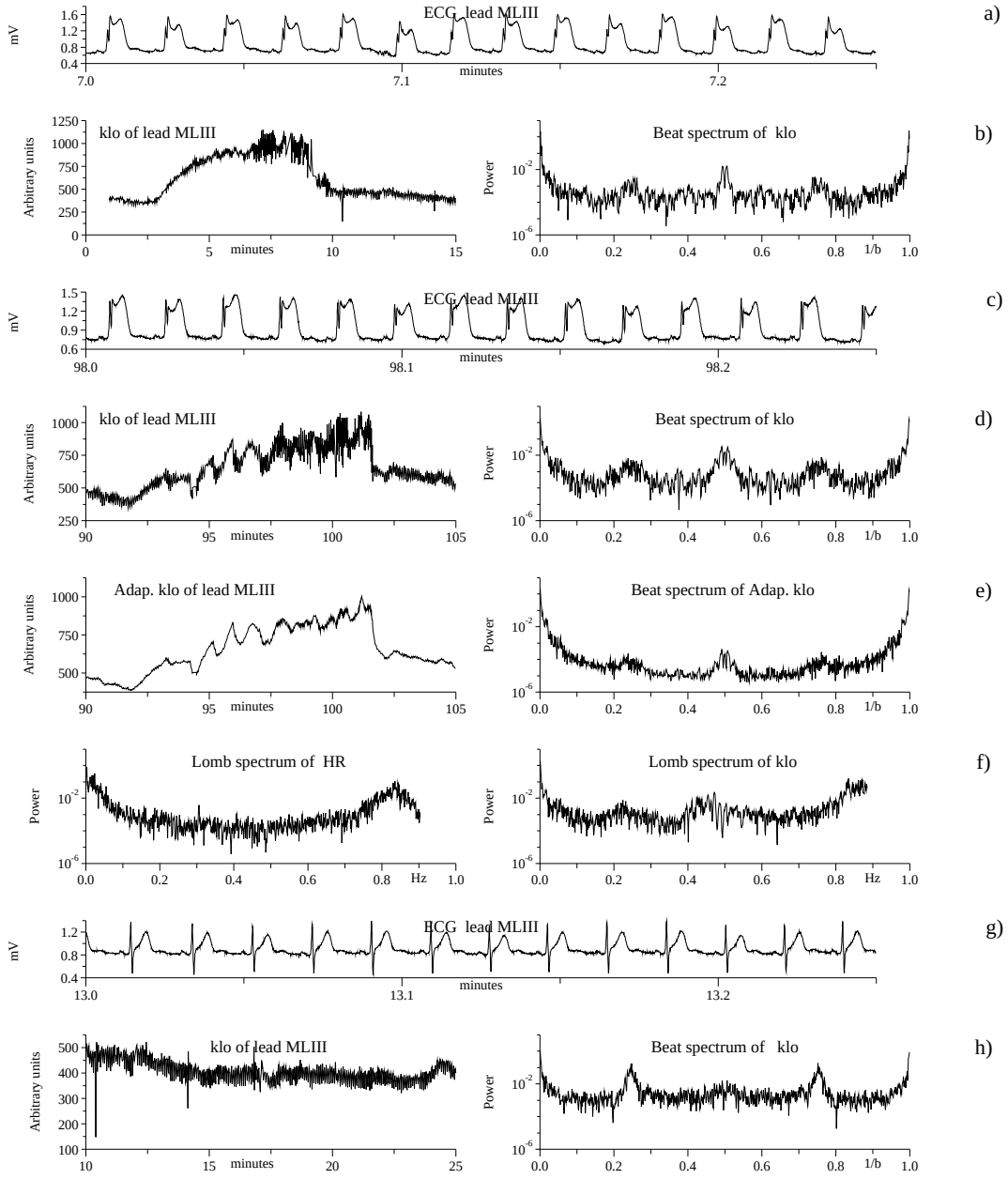


Figure 11: *Alternans in record e0105 of the European ST-T Database. Panel (a) illustrates the ECG during the first ischemic ST-T episode; (b) shows the $kl_0(i)$ time series during a 15-minute interval including the ischemic episode, and the corresponding beat spectrum. The beat spectrum exhibits a clear peak corresponding to period 2 alternans (at 0.5 $b^{-1}$), and also shows period 4 alternans (at 0.25 $b^{-1}$). Panel (c) shows an excerpt of the ECG during another ischemic episode; (d) shows the corresponding $kl_0(i)$ time series and beat spectrum, and (e) shows the same data, derived using adaptive estimation. The adaptive estimate attenuates the beat-to-beat variations; it is better suited for study of longer-term variations. Panel (f) shows the HR power spectrum and the $kl_0(i)$ frequency spectrum for the same interval (see text). Panels (g) and (h) show an excerpt of ECG, a $kl_0(i)$ time series, and the corresponding beat spectrum during a non ischemic period in the same record, where the period 2 alternans has disappeared, but a period 4 alternans remains.*